International Journal of Mathematics and Statistics Studies, 12 (5), 54-66, 2024

Print ISSN: 2053-2229 (Print),

Online ISSN: 2053-2210 (Online)

Website: https://www.eajournals.org/

Publication of the European Centre for Research Training and Development -UK

Impact of Thermal and Hemodynamic Factors on Blood Flow in Magnetized Arteries: A Mathematical Perspective

J.K. Butter[1*] A.P. Miller[2], S.S. Obonin[3]
[1,2,3]Department of Mathematics and Statistics, Federal University Otuoke, Bayelsa State.
[1]Nigerian Society for Mathematical Biology (NSMB).
butter@mail.yu.edu

doi: https://doi.org/10.37745/ijmss.13/vol12n55466 Published December 30, 2024

Citation: Butter J.K., Miller A.P., and Obonin S.S. (2024) Impact of Thermal and Hemodynamic Factors on Blood Flow in Magnetized Arteries: A Mathematical Perspective, *International Journal of Mathematics and Statistics Studies*, 12 (5), 54-66

ABSTRACT: *Maintaining optimal blood pressure is vital for overall health, as deviations from normal levels can lead to serious complications. Hypertension is known to damage the cardiovascular system and vital organs, while hypotension reduces blood flow, impairing critical bodily functions. Effective management strategies, such as lifestyle modifications, regular monitoring, and medical interventions, are crucial in mitigating these risks. Mathematical modeling plays an integral role in analyzing blood circulation in the human body. By translating real-world cardiovascular challenges into mathematical equations, it enables the study of complex physiological systems. In this research, the combined effects of heat and blood pressure on blood flow through blood vessels were modeled mathematically. The Navier-Stokes equation was modified to develop a system of partial differential equations (PDEs) governing blood momentum and temperature distribution. The system of PDEs was then scaled into a set of dimensionless models and further simplified into Ordinary Differential Equations (ODEs) using oscillatory perturbation parameters. Laplace transformation techniques were employed to solve the governing equations analytically. The resulting flow profiles were simulated numerically using Wolfram Mathematica (Version 12), with variations in key biophysical parameters. key findings from the simulation include: An increase in the Prandtl number resulted in decreased temperature and velocity profiles. A rise in the Grashof number led to an enhancement in blood velocity. Increasing the oscillatory frequency exhibited a diminishing effect on both temperature and velocity profiles.*

KEY WORDS: Blood Pressure, Temperature, Magnetic field, Artery, Hypertension, hypotension, cardiovascular diseases.

INTRODUCTION

Blood flow dynamics in the human body is a complex process influenced by a myriad of physiological and environmental factors (Bunonyo et al., 2024). Proper blood pressure regulation is essential for health, as deviations from normal levels can lead to critical conditions. Hypertension can damage the cardiovascular system and vital organs, while hypotension impairs blood flow, leading to the disruption of essential body functions. Among the health risks associated with abnormal blood pressure are kidney damage, heart attacks, and other cardiovascular diseases.

One critical area of study is the interaction between temperature gradients, fluid pressure, and external forces, such as magnetic fields, on blood flow in microchannels, including capillaries and small arteries. Blood flow is essential for nutrient transport, waste removal, and thermoregulation in the human body (Butter et al., 2024). Mathematical modeling of blood flow is invaluable for studying these processes, enabling the development of medical interventions such as drug delivery systems and magnetic resonance imaging (MRI)-guided therapies (Akbar & Shah, 2024).

Blood vessel narrowing also known as stenosis, caused by plaque buildup (a combination of cholesterol and cells) disrupts blood circulation and heart function, increasing the risk of heart failure. This narrowing not only restricts oxygen-rich blood flow but also affects the temperature, pressure, and speed of blood flow through the vessel (Yusuf et al., 2016). Previous studies have explored the implications of stenosis on blood flow dynamics. For example, Plourde et al. (2015) used numerical simulations to examine how plaque clearance impacts pressure drop and flow velocity, while Maruthi (2015) investigated the effects of stenosis and post-stenotic expansion on Jeffrey's fluid flow in vessels. Kabir (2021) developed computational models to study blood flow in normal arteries and arteries with stenosis, revealing that fluid properties peak at the stenosis site and magnify with increasing vessel narrowing.

Temperature also plays a crucial role in blood flow dynamics, as it influences viscosity and thermal conductivity. Elevated temperatures reduce blood viscosity, enhancing velocity, while lower temperatures slow down blood movement (Bunonyo et al., 2024). Temperature gradients can induce thermophoretic effects, altering the motion of particles or solutes in blood and affecting flow profiles. Misra and Sinha (2013) studied the effects of temperature radiation on magnetohydrodynamic (MHD) fluid movement, while Abubakar and Adeoye (2020) explored the role of thermal radiation and magnetic fields in blood flow through tapering stenosed permeable channels.

Blood plasma contains various ions like sodium, potassium, calcium, and chloride, which make the blood electrically conductive. these charges experience Lorentz forces, leading to changes in blood flow dynamics. Magnetic fields significantly affect blood flow due to the paramagnetic properties of hemoglobin, the oxygen-carrying molecule in red blood cells. Various researchers have studied these effects, including Yadav and Roshan (2024), who conducted computational simulations of blood flow in a circular porous zone, and Sharma et al. (2023), who examined MHD hemodynamics in stenosed arterial channels. Oyelami et al. (2021) investigated the thermal effects of magnetic fields on symmetrical stenotic arterial blood circulation, while Rashidi et al. (2014) analyzed MHD fluid behavior in spinning permeable vessels.

Despite significant progress, there remain gaps in understanding the combined effects of temperature, pressure, and magnetic fields on blood flow, especially in stenosed vessels. This study aims to address these gaps by developing a mathematical model to analyze the thermo-pressure effects on blood flow in the presence of a magnetic field. The findings could enhance biomedical device design and therapeutic strategies, including hyperthermia treatments and magnetic drug targeting.

MATHEMATICAL FORMULATION

Let's consider the following assumptions: The flow is axial; the tangential velocity is assumed to be zero; the fluid is blood, incompressible, and viscous; the viscosity is constant throughout the fluid medium; the fluid is influenced by the pressure gradient of the fluids; there is no electrical conductivity in the system; we considered the effect of an external magnetic field; and the blood vessel is porous; the flow obeys the no-slip condition. The mathematical model system is presented based on the assumptions made above and previous research by Butter et al. (2024), Bunonyo et al. (2018), Bunonyo and Amos (2023), Hanvey & Bunonyo (2022), and Verma and Parihar (2010).

Following the thermal volumetric expansion according to Bunonyo *et al.* (2018), we have:

$$\rho_b + \rho_\infty = \rho_b \beta_T \left(T^* - T_\infty\right) \tag{1}$$

Momentum equation

Following the aforementioned assumption and the works of Bunonyo & Ndu (2024) and Verma and Parihar (2010), we present the momentum equation as:

$$\rho_b \frac{\partial w^*}{\partial t} = \mu_b \left(\frac{\partial^2 w^*}{\partial r^{*2}} + \frac{1}{r^*}\frac{\partial w^*}{\partial r^*} \right) + \rho_b \vec{g}_\infty \beta_T \left(T^* - T_\infty\right) - \frac{\partial P^*}{\partial x^*} + \vec{J} \times \vec{B} \tag{2}$$

Heat equation

Following Bunonyo et al. 2018, the heat equation is:

$$\rho_b c_{bp} \frac{\partial T^*}{\partial t^*} = k_{Tb} \left(\frac{\partial^2 T^*}{\partial r^{*2}} + \frac{1}{r^*}\frac{\partial T^*}{\partial r^*} \right) \tag{3}$$

The equivalent initial and boundary conditions are:

$$\left.\begin{array}{l} w^* = 0,\ T^* = T_w \ \text{ at } r^* = R < \infty \\ w^* \neq 0,\ T^* = T_\infty \ \text{ at } r^* = 0 \end{array}\right\} \tag{4}$$

DIMENSIONLESS QUANTITIES

$$\left.\begin{array}{l} x=\dfrac{x^*}{\lambda}, r=\dfrac{r^*}{R_0}, \upsilon_b=\dfrac{\mu_b}{\rho_b}, w=\dfrac{w^* R_0}{\upsilon_b}, t=\dfrac{t^*\upsilon_b}{R_0^2}, P=\dfrac{R_0^3 P^*}{\upsilon_b \mu_b \lambda}, \dfrac{\partial P^*}{\partial x^*}=\rho_\infty \vec{g}_x, \\ Gr=\dfrac{\vec{g}_x \beta_T \left(T_w-T_\infty\right) R_0^3}{\upsilon_b^2}, \theta=\dfrac{T^*-T_\infty}{T_w-T_\infty}, Pr=\dfrac{\mu_b c_{bp}}{k_{Tb}}, P_0=\dfrac{\partial P}{\partial x}, M=B_0 R_0\sqrt{\dfrac{\sigma_{eb}}{\mu_b}} \end{array}\right\} \quad (5)$$

Scaling equation (2) – (4) using the dimensionless quantities in equation (5), we have:

$$\frac{\partial w}{\partial t}=-\frac{\partial P}{\partial x}+\left(\frac{\partial^2 w}{\partial r^2}+\frac{1}{r}\frac{\partial w}{\partial r}\right)+\theta Gr-M^2 w \quad (6)$$

$$Pr\frac{\partial \theta}{\partial t}=\frac{\partial^2 \theta}{\partial r^2}+\frac{1}{r}\frac{\partial \theta}{\partial r} \quad (7)$$

The corresponding initial and boundary conditions are:

$$\left.\begin{array}{ll} w=0,\ \theta=1, & \text{at } r=h<\infty \\ w\neq 0,\ \theta=0, & \text{at } r=0 \end{array}\right\} \quad (8)$$

PERTURBATION SOLUTION

The flow in the blood channel is oscillatory due to the heart rate, hence, the flow profiles are assumed as:

$$\left.\begin{array}{l} w=w_0 e^{\omega t} \\ \theta=\theta_0 e^{\omega t} \\ \dfrac{dP}{dx}=P_0 e^{\omega t} \end{array}\right\} \quad (9)$$

Applying equation (9) on equations (6) - (8), we have:

$$\frac{d^2 w_0}{dr^2}+\frac{1}{r}\frac{dw_0}{dr}-M^2 w_0=P_0-Gr\theta_0 \quad (10)$$

$$\frac{d^2 \theta_0}{dr^2}+\frac{1}{r}\frac{d\theta_0}{dr}-\lambda_2^2\theta_0=0 \quad (11)$$

The corresponding initial and boundary conditions are:

$$\left.\begin{array}{ll} w_0=0, \theta_0=e^{-\omega t} & \text{at } r=h<\infty \\ w_0\neq 0, \theta_0=0 & \text{at } r=0 \end{array}\right\} \quad (12)$$

where: $\lambda_2^2=Pr\omega$,

METHOD OF SOLUTION

We shall be stating the Laplace of the profiles mathematically as:

$$\left.\begin{array}{l} L\{w(r)\} = w(s) = \int_0^\infty w(r)e^{-sr}dr \\ L\{\theta(r)\} = \theta(s) = \int_0^\infty \theta(r)e^{-sr}dr \end{array}\right\} \quad (13)$$

Applying equation (13) on equation (11), we have:

$$\frac{d\theta_0}{\theta_0} = -\frac{s}{\left(s^2-\lambda_2^2\right)}ds \quad (14)$$

Further simplification by integrating equation (14), we have:

$$\theta_0(s) = \frac{A}{\sqrt{\left(s^2-\lambda_2^2\right)}};\ A \subset \square \quad (15)$$

Note that, if $L\{\theta_0(r)\} = \theta_0(s)$, then

$$\theta_0(r) = L^{-1}\{\theta_0(s)\} = AL^{-1}\left\{\frac{1}{\sqrt{\left(s^2-\lambda_2^2\right)}}\right\} = AI_0(\lambda_2 r) \quad (16)$$

where $I_0(\lambda_2 r)$ is the modified Bessel function of order zero. Using the boundary conditions in equation (12), we get the constant coefficient as:

$$A = \frac{1}{I_0(\lambda_2 h)e^{\omega t}} \quad (17)$$

Putting equation (17) into equation (16), we have:

$$\theta_0(r) = \frac{I_0(\lambda_2 r)}{I_0(\lambda_2 h)e^{\omega t}} \quad (18)$$

where $I_0(\lambda_2 r) = \left(1 + \frac{\lambda_2^2 r^2}{4} + \frac{\lambda_2^4 r^4}{64} + \ldots\right)$ and $I_0(\lambda_2 h) = \left(1 + \frac{h^2\lambda_2^2 r^2}{4} + \frac{h^4\lambda_2^4 r^4}{64} + \ldots\right)$

Substituting equation (18) into equation (9), we have the temperature profile as:

$$\theta(r) = \frac{1}{I_0(\lambda_2 h)}\left(1 + \frac{\lambda_2^2 r^2}{4} + \frac{\lambda_2^4 r^4}{64} + \ldots\right) \quad (19)$$

Substituting equation (18) into the momentum equation (10) and presenting with a particular term, we have:

$$r\frac{d^2 w_{0p}}{dr^2} + \frac{dw_{0p}}{dr} - rM^2 w_{0p} = r\beta_3 + \frac{\beta_2^2\lambda_2^2 r^3}{4} + \frac{\beta_2^2\lambda_2^4 r^5}{64} \quad (20)$$

where $\beta_2^2 = -\dfrac{Gr}{I_0(\lambda_2 h)e^{\omega t}}, \beta_3^2 = P_0 - \beta_2^2$

let the particular solution be in the form:

$$w_{0p} = A_0 + A_1 r + A_2 r^2 + A_3 r^3 + A_4 r^4 + A_5 r^5 \tag{21}$$

Solving equation (20), we get:

$$\left.\begin{aligned} A_0 &= -\frac{\beta_3^2}{M^2} - \frac{\beta_2^2}{M^4}\left(\lambda_2^4 + \lambda_2^2\right),\ A_1 = 0 \\ A_2 &= -\frac{\beta_2^2}{4M^2}\left(\lambda_2^4 + \lambda_2^2\right), A_3 = 0 \\ A_4 &= -\frac{\beta_2^2 \lambda_2^4}{M^2 64}, A_5 = 0 \end{aligned}\right\} \tag{22}$$

Substituting equation (22) into equation (21), we get:

$$w_{0p} = -\frac{\beta_3^2}{M^2} - \frac{\beta_2^2}{M^4}\left(\lambda_2^4 + \lambda_2^2\right) - \frac{\beta_2^2}{4M^2}\left(\lambda_2^4 + \lambda_2^2\right) r^2 - \frac{\beta_2^2 \lambda_2^4}{64M^2} r^4 \tag{23}$$

The homogeneous solution of equation (20) is: $w_{0h} = BI_0(\lambda_2 r)$ (24)

homogeneous solution plus the particular solution gives the general solution of equation (20), which is:

$$w_0 = BI_0(\lambda_2 r) - \frac{\beta_3^2}{M^2} - \frac{\beta_2^2}{M^4}\left(\lambda_2^4 + \lambda_2^2\right) - \frac{\beta_2^2}{4M^2}\left(\lambda_2^4 + \lambda_2^2\right) r^2 - \frac{\beta_2^2 \lambda_2^4}{64M^2} r^4 \tag{25}$$

Using the initial and boundary conditions in equation (8), we get:

$$B = \frac{\beta_3^2}{M^2 I_0(\lambda_2 h)} + \frac{\beta_2^2}{M^4 I_0(\lambda_2 h)}\left(\lambda_2^4 + \lambda_2^2\right) + \frac{\beta_2^2}{4M^2 I_0(\lambda_2 h)}\left(\lambda_2^4 + \lambda_2^2\right) h^2 + \frac{\beta_2^2 \lambda_2^4}{64M^2 I_0(\lambda_2 h)} h^4$$

Substituting equation (25) into equation (9), we get:

$$w(r,t) = BI_0(\lambda_2 r) - \frac{\beta_{31}^2}{M^2} - \frac{\beta_{21}^2}{M^4}\left(\lambda_2^4 + \lambda_2^2\right) - \frac{\beta_{21}^2}{4M^2}\left(\lambda_2^4 + \lambda_2^2\right) r^2 - \frac{\beta_{21}^2 \lambda_2^4}{64M^2} r^4 \tag{26}$$

where $\beta_{21}^2 = -\dfrac{Gr}{I_0(\lambda_2 h)}$, $\beta_{31}^2 = P_0 e^{\omega t} - \dfrac{Gr}{I_0(\lambda_2 h)}$

$$B = \frac{\beta_{31}^2}{M^2 I_0(\lambda_2 h)} + \frac{\beta_{21}^2}{M^4 I_0(\lambda_2 h)}\left(\lambda_2^4 + \lambda_2^2\right) + \frac{\beta_{21}^2}{4M^2 I_0(\lambda_2 h)}\left(\lambda_2^4 + \lambda_2^2\right) h^2 + \frac{\beta_{21}^2 \lambda_2^4}{64M^2 I_0(\lambda_2 h)} h^4$$

PRESENTATION OF RESULTS

Haven obtained the analytical solution to the formulated problem, we carried out a numerical simulation using Wolfram Mathematica version 12 and in order to validate the analytical solution, the parameters data were obtained from previous research carried out by Bunonyo et al. (2024), Bunonyo *et al*. (2021), and Hanvey and Bunonyo (2022), respectively. The results are presented as follows:

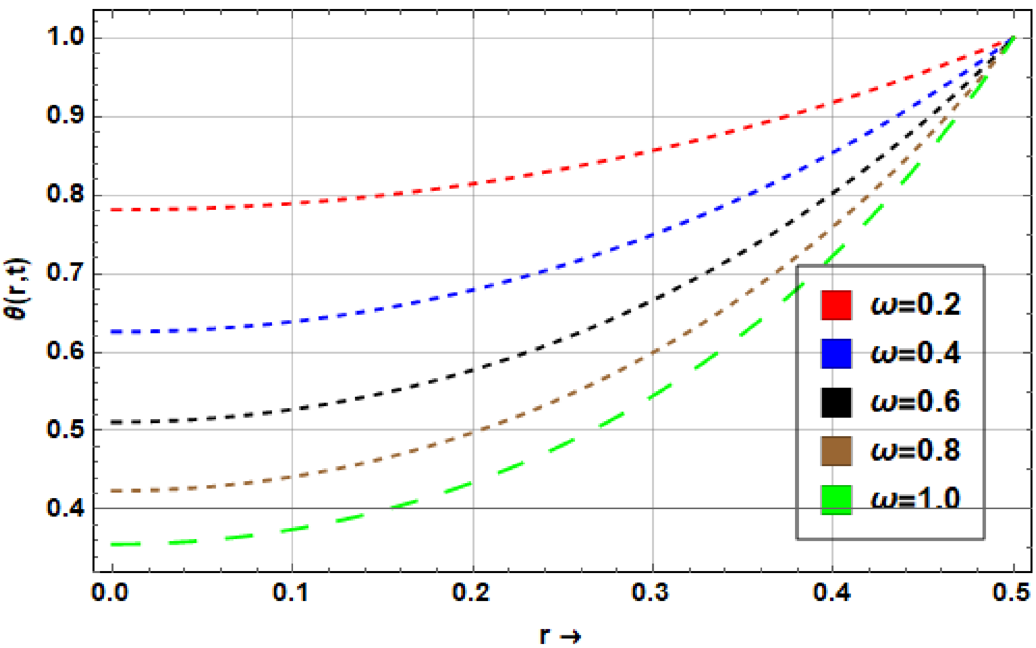

Figure 1: The effect of oscillation frequency on the fluid temperature

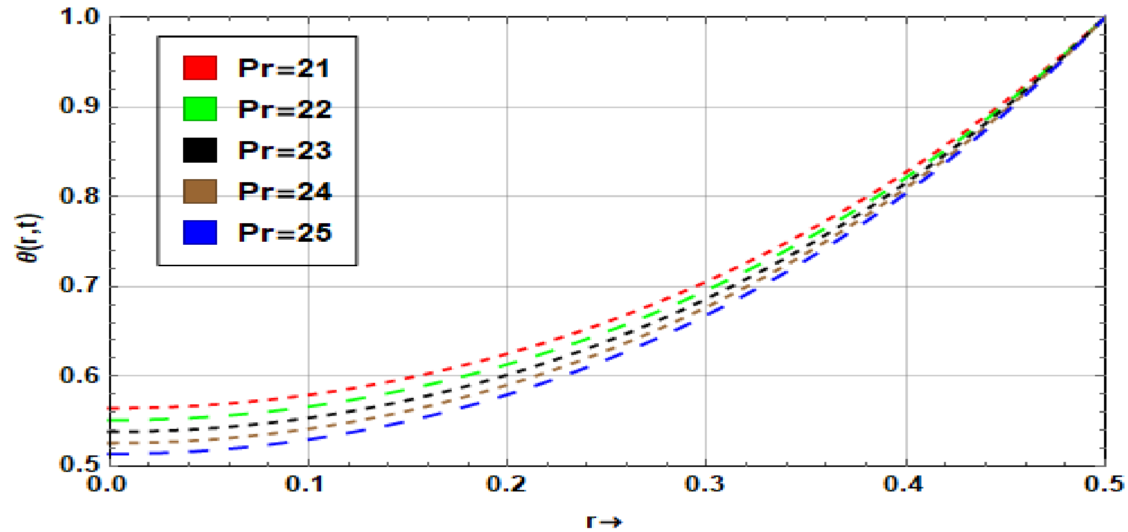

Figure 2: The effect of Prandtl frequency on the fluid temperature

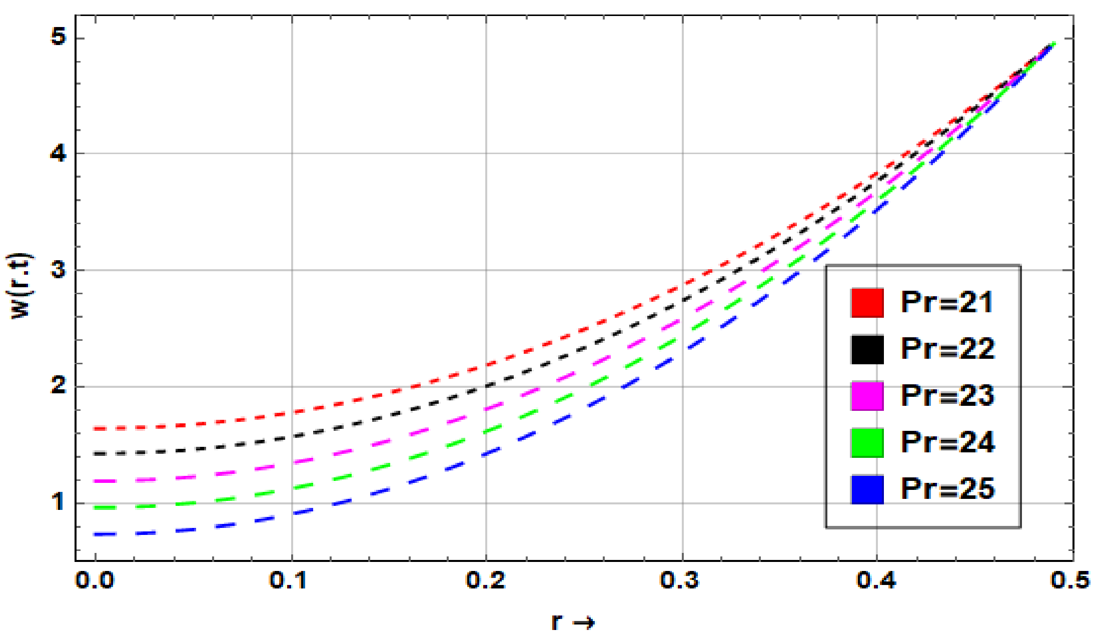

Figure 3: The effect of Prandtl number on the fluid velocity

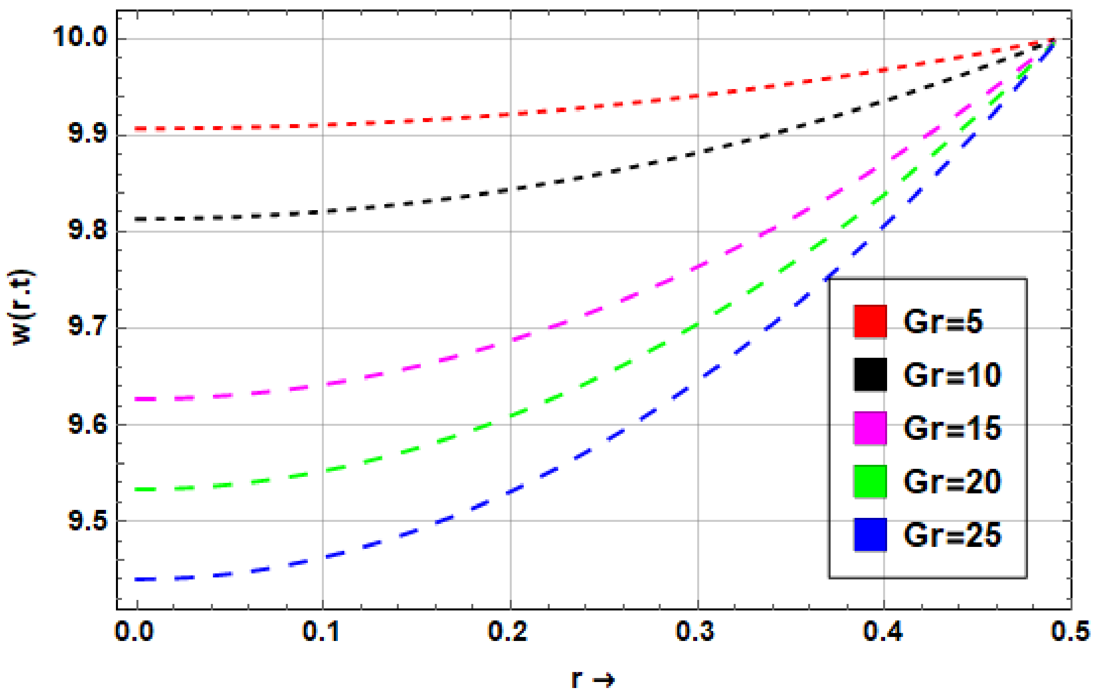

Figure 4: The effect of Grashof number on the fluid velocity

DISCUSSION OF RESULT

The graphical result as seen in **figure 1** depicts the effect of the oscillatory number $\omega = 0.2, 0.4, 0.6, 0.8, 1.0$ where the Prandtl number $\Pr = 21$ and the blood pressure $P_0 = 120 mmHg$ on the fluid temperature. The result is of the view that the temperature was maximum when the boundary layer width was zero and raised to the peak at maximum thickness. A decrease in temperature profile was noticed before increasing to its peak. **Figure 2** and **3** indicated a reduction in fluid temperature and blood velocity respectively as the oscillatory frequency $\omega = 0.2$, blood pressure $P_0 = 120 mmHg$ and Prandtl number increased by $\Pr = 21, 22, 23, 24, 25$. However, it was also seen that the temperature and fluid velocity began to rise as the boundary layer expanded until it reached its maximum. **Figure 4** is of the opinion that when the Prandtl number is kept at $\Pr = 21$, blood pressure kept at $P_0 = 120 mmHg$, oscillatory frequency $\omega = 0.2$, and the Grashof number was increased $Gr = 15, 20, 25, 30, 35$, the blood velocity was maximum when the boundary layer width was zero and grew to the peak at maximum thickness. A decrease in velocity profile was noticed before increasing to its peak.

CONCLUSION

This study investigated the effects of temperature and pressure on blood flow in the presence of a magnetic force using a mathematical modeling approach. The governing equations were developed and solved analytically, followed by numerical simulations. The results were presented, discussed, and summarized, leading to the following conclusions:

1. Increasing the Prandtl number led to a decrease in both temperature and velocity, indicating that higher Prandtl numbers reduce heat and momentum transfer efficiency.
2. A rise in the Grashof number enhanced blood velocity, demonstrating the role of buoyancy forces in augmenting flow within the microchannel.
3. Variations in oscillatory frequency showed a diminishing effect on both temperature and velocity.
4. Blood pressure variations ($P_0 = 120mmHg$) acted as a driving force for maintaining flow stability.

FUTURE RESEARCH

For further studies, we recommend extended research to include the interaction of blood flow with the elastic walls of vessels, to simulate realistic vascular conditions.

NOMENCLATURE

w^*, u^* Dimensional blood velocity in different directions
x^*, r^* Dimensional axial and radial distances
T^* Dimensional blood temperature
P Dimensionless blood pressure
T_∞ Far field Dimensional blood temperature
T_w Dimensionless wall temperature
w Dimensionless blood velocity
w_0 Perturbed blood velocity
ρ_b Blood density
μ_b Blood viscosity
ΣF Sum of forces acting on the fluid in circulation
c_{bp} Blood specific heat capacity
ω Oscillatory frequency
t Dimensionless time

B Magnetic induction
k^* Permeability
k Porosity
B_0 Magnetic field intensity
θ Dimensionless temperature
k_T Thermal conductivity
μ Dynamic viscosity of the blood
k_{Tb} Blood thermal conductivity
k_0 Chemical Reactant
ω Oscillation frequency
Pr Prandtl number
Gr Grashof number
Da Darcy number
Sr Soret number
g Acceleration due to gravity

β_T Volumetric temperature expansion rate.

REFERENCES

Abubakar, J. U., & Adeoye, A. D. (2020). Effects of radiative heat and magnetic field on blood flow in an inclined tapered stenosed porous artery. *Journal of Taibah University for Science*, 14(1), 77-86.

Akbar, S., & Shah, S. R. (2024). Mathematical Modeling of Blood Flow Dynamics in the Cardiovascular System: Assumptions, Considerations, and Simulation Results. *Journal of Current Medical Research and Opinion*, 7(04), 2216-2225.

Bunonyo, K. W., & Ebiwareme, L. (2022). A low Prandtl number haemodynamic oscillatory flow through a cylindrical channel using the Power Series Method. *European Journal of Applied Physics,* 4(3), 56-65.

Bunonyo, K. W., & Ndu, R. I. (2024) Mathematical Modelling and Numerical Simulation of Haematocrit and Pressure Effects on Blood Flow through Blood Vessel. *International Research Journal of Pure and Applied Physics,* 11 (1),132-143

Bunonyo, K. W., Amos, E., & Eli, I. C. (2018). Unsteady oscillatory couette flow between vertical parallel plates with constant radiative heat flux. *Asian Research Journal of Mathematics*, *11*(2), 1-11.

Butter, J. K., Bunonyo, K. W., & Eli, I. C. (2024). Mathematical Modelling of the Thermosolutal Effect on Blood Flow through a Micro-Channel in the Presence of a Magnetic Field. *British Journal of Multidisciplinary and Advanced Studies,* 5(4), 14-32.

Fahim, M., Sajid, M., & Ali, N. (2024). Pulsatile pressure-driven non-Newtonian blood flow through a porous stenotic artery: A computational analysis. *Numerical Heat Transfer, Part A: Applications*, 1-21.

Joshua, T. M., Anwar, K., & Abdullah, N. (2020, June). Numerical study of magnetohydrodynamic blood flow through an artery with multiple stenosis. In IOP Conference Series: *Materials Science and Engineering (*Vol. 864, No. 1, p. 012199). *IOP Publishing*.

K. W. Bunonyo, J. K. Butter, I. C. Eli (2024), Modelling and Simulation of the Effect of Prandtl and Soret Numbers on Mass Concentration with Magnetic Intensity in a Blood Channel. *African Journal of Mathematics and Statistics Studies* 7(3), 143-155. DOI: 10.52589/AJMSS-A7NIEBYY

Kabir, M. A., Alam, M. F., & Uddin, M. A. (2021). Numerical simulation of pulsatile blood flow: a study with normal artery, and arteries with single and multiple stenosis. *Journal of Engineering and Applied Science*, 68, 1-15.

Maruthi Prasad, K., Bhuvana Vijaya, R. & Umadevi, C. (2015) Effects of Stenosis and Post Stenotic Dilatations on Jeffrey Fluid Flow in Arteries. *International Journal of Research in Engineering and Technology,* 4, 195-201.

Misra, J. C., & Sinha, A. (2013). Effect of thermal radiation on MHD flow of blood and heat transfer in a permeable capillary in stretching motion. *Heat and Mass Transfer*, 49, 617-628.

Omamoke, E., Amos, E., & Jatari, E. (2020). Impact of thermal radiation and heat source on MHD blood flow with an inclined magnetic field in Treating Tumor and Low Blood Pressure. *Asian Research Journal of Mathematics*, 16(9), 77-87.

Oyelami, F. H., Ige, E. O., Taiyese, N. O., & Saka-Balogun, O. Y. (2021). Magneto-radiative analysis of thermal effect in symmetrical stenotic arterial blood flow. *Journal of Mathematic and Computational Science* 11(5), 5213-5230.

Plourde, B. D., Vallez, L. J., Sun, B., Abraham, J. P., & Staniloe, C. S. (2015). The effect of plaque removal on pressure drop and flow rate through an idealized stenotic lesion. *Biology and Medicine*, 8, 261.

Rashidi, M. M., Kavyani, N., & Abelman, S. (2014). Investigation of entropy generation in MHD and slip flow over a rotating porous disk with variable properties. *International Journal of Heat and Mass Transfer,* 70, 892-917.

Sharma, B. K., Gandhi, R., Abbas, T., & Bhatti, M. M. (2023). Magnetohydrodynamics hemodynamics hybrid nanofluid flow through inclined stenotic artery. *Applied Mathematics and Mechanics*, 44(3), 459-476.

Venkatesan, J., Sankar, D. S., Hemalatha, K., & Yatim, Y. (2013). Mathematical analysis of Casson fluid model for blood rheology in stenosed narrow arteries. *Journal of Applied Mathematics,* 2013(1), 583809.

Verma, N., & Parihar, R. S. (2010). Mathematical model of blood flow through a tapered artery with mild stenosis and hematocrit. *Journal of Modern Mathematics & Statistics* 4(1), 38-43

Yadav, P. K., & Roshan, M. (2024). Mathematical modeling of blood flow in an annulus porous region between two coaxial deformable tubes: An advancement to peristaltic endoscope. *Chinese Journal of Physics,* 88, 89-109.